Received: 16 November 2023 | Accepted: 3 April 2024

DOI: 10.1002/iub.2828

RESEARCH ARTICLE

IUBMB LIFE WILEY

Functional and biochemical characterisation of remote homologues of type IV pili proteins PilN and PilO in *Helicobacter pylori*

Sharmin Q. Bonny[1] | **Xiaotian Zhou**[1] | **Mohammad F. Khan**[1] | **Mohammad M. Rahman**[1] | **Yue Xin**[1] | **Naveen Vankadari**[1] | **Alexandra Tikhomirova**[1] | **Jihane Homman-Ludiye**[2] | **Anna Roujeinikova**[1,3]

[1]Department of Microbiology, Infection and Immunity Program, Monash Biomedicine Discovery Institute, Monash University, Melbourne, Victoria, Australia

[2]Monash Micro Imaging, Biomedicine Discovery Institute, Monash University, Melbourne, Victoria, Australia

[3]Department of Biochemistry and Molecular Biology, Monash University, Melbourne, Victoria, Australia

Correspondence
Anna Roujeinikova, Department of Microbiology, Infection and Immunity Program, Monash Biomedicine Discovery Institute, Monash University, Melbourne, Victoria 3800, Australia.
Email: anna.roujeinikova@monash.edu

Funding information
Australian Research Council, Grant/Award Number: DP210103056

Abstract

Helicobacter pylori encodes homologues of PilM, PilN and PilO from bacteria with Type IV pili, where these proteins form a pilus alignment complex. Inactivation of *pilO* changes *H. pylori* motility in semi-solid media, suggesting a link to the chemosensory pathways or flagellar motor. Here, we showed that mutation of the *pilO* or *pilN* gene in *H. pylori* strain SS1 reduced the mean linear swimming speed in liquid media, implicating PilO and PilN in the function, or regulation of, the flagellar motor. We also demonstrated that the soluble variants of *H. pylori* PilN and PilO share common biochemical properties with their Type IV pili counterparts which suggests their adapted function in the bacterial flagellar motor may be similar to that in the Type IV pili.

KEYWORDS

bacterial flagellar motor, *Helicobacter pylori*, motility, oligomeric state, type IV pili

1 | INTRODUCTION

Helicobacter pylori infections are associated with chronic gastritis and peptic ulcers which can lead to the development of gastric cancer.[1–4] *H. pylori* is the leading cause of cancer attributed to infectious agents,[5] and gastric cancer ranks fourth in terms of mortality.[6] The major virulence factors of *H. pylori* include secreted toxins that cause pathological changes in the epithelial cells.[7–9] *H. pylori* also modifies its local environment to be able to withstand the acidic pH of the stomach,[10] defends itself against the host innate immune response by degrading innate immune peptides,[11] detoxifies reactive oxygen species produced by leukocytes,[12] and camouflages its surface-exposed proteins via glycosylation.[13] Motility by flagella is key to finding critical nutrients and molecules that protect bacteria from elimination by host complement.[14–16] The flagellar motor is significantly larger and more complex in *H. pylori* in comparison to *E. coli* and *Salmonella*.[17] It contains a large

Sharmin Q. Bonny and Xiaotian Zhou made equal contributions.

periplasmic scaffold that anchors the force-generating stator units and stabilises the wider stator ring to sustain a larger turning force.[18] The energy released upon binding of the stator units to the scaffold is thought to promote their activation via interlinked conformational changes.[19–22]

Although it is now recognised that polar flagellar motors in many other bacteria are similarly complex,[18,23] our understanding of how the assembly and function of this intricate machine is regulated is still in its infancy. Identification of motor components in *H. pylori* often cannot be achieved solely by genome analysis, because the bacterium does not group all flagellar genes into common operons.[24] A different approach (extragenic suppressor analysis) has recently led to a discovery that the soft-agar motility defect of the *H. pylori* strain G27 lacking the chemotaxis gene *cheV1* was reduced by suppressor mutations in the gene HPG27_252 encoding a distant homologue of the Type IV pili protein PilO.[25] Deletion of HPG27_252 similarly resulted in partial recovery of the soft-agar motility phenotype. The PilO homolog was thus identified as a new protein with a function associated with regulation of migration in semi-solid media. The *H. pylori pilO* gene is co-transcribed with the genes encoding homologs of Type IV pili proteins PilM and PilN (Figure 1A).[25,26] PilM, PilN and PilO form the Type IV pilus alignment complex.[27–29] The discovery of PilM, PilN and PilO in *H. pylori*[25] is intriguing because *H. pylori* does not possess Type IV pili. The apparent association with regulation of migration in soft agar is an interesting lead. Recognising that the diameter of swimming halos in agar can have various causes (e.g., viscosity, surface sensing), we wished to determine if the swimming speed is directly impacted when the genes encoding the membrane-anchored, periplasm-oriented proteins components PilN and PilO are mutated. We therefore assessed the effect of inactivation of these genes on the linear swimming speed of *H. pylori* strain SS1 in liquid medium. Having established that mutants swim slower than wild-type cells, we generated and tested different expression constructs for the periplasmic moieties of *H. pylori* PilN and PilO, developed methods for production of pure recombinant forms of these proteins for functional and structural studies, and compared their behaviour in solution to those of PilN and PilO from Type IV pili.

2 | MATERIALS AND METHODS

The *H. pylori* strain SS1 Δ*pilN::kan* and Δ*pilO::kan* mutants were created by replacing the middle part of *pilN* (locus tag HPYLSS1_00261) or *pilO* (locus tag HPYLSS1_00262) gene with the *Campylobacter coli* kanamycin resistance gene *aphA3* (Genbank ID HG515011.2). DNA fragments containing *aphA3*, flanked by *H. pylori* chromosomal DNA sequences corresponding to 200 bp upstream plus the first 100 bp of the targeted gene, and the last 100 bp plus 200 bp downstream of the targeted gene, were synthesized and ligated into pUC18 by GenScript (USA). The Δ*pilN* and Δ*pilO* mutants were generated using natural transformation.

The swimming behaviour of the strains cultured in BB10 (Brucella broth supplemented with 10 μg/mL vancomycin and 10% [v/v] foetal bovine serum) was filmed using a Leica DMi8 microscope in a bright-field mode at 20× magnification. Five 30-sec videos (16 frames per second) were captured for each strain, in three independent biological replicates. The videos were analysed using ImageJ v.1.53. For each strain, a total of 66 cells that swam in linear fashion for at least 0.5 s were tracked manually using the MTrack plug-in to allow calculation of the mean straight swimming speed. GraphPad Prism (version 10.1.2) was used to carry out one-way analysis of variance (ANOVA) followed by Dunnett's test to calculate *p*-values and determine statistical significance of the observed swimming speed differences between the WT and mutants.

The membrane topologies and structures of PilN and PilO were predicted using TOPCONS (http://topcons.net/)[30] and AlphaFold2.[31,32] To generate vectors for expression of N-terminally His_6-tagged variants that lack the transmembrane helix ($PilN_{41}$ and $PilO_{45}$), the coding sequences for PilN residues 41–177 or PilO residues 45–179 were synthesized and ligated into the pET151/D-TOPO vector (Invitrogen) by GenScript, with the nucleotides encoding the His_6 tag and tobacco etch virus (TEV) protease cleavage site at the 5′ end. Vectors for expression of only the C-terminal globular domains of PilN ($PilN_{88}$, residues 88–177) and PilO ($PilO_{95}$, residues 95–179) with a cleavable N-terminal His_6-tag were generated by the same principle. To produce a vector for expression of $PilO_{45}$ with a C-terminal His_6-tag, the gene encoding residues 45–179 was inserted into the pET22-b(+) vector.

$PilN_{88}$ and $PilO_{95}$ were expressed in soluble forms in *E. coli* BL21(DE3) at 16°C in LB with 50 μg/mL ampicillin, with overnight expression with 0.1 mM IPTG. $PilN_{41}$ and $PilO_{45}$ were expressed in inclusion bodies (IBs) (37°C, 4 h). To prepare IBs for protein refolding trials, the cell pellet was resuspended in buffer A (10 mM Tris–HCl pH 8.0, 100 mM NaCl), lysed using an Avestin EmulsiFlex-C5 high-pressure homogenizer (Avestin) and centrifuged at 10,000 × *g* for 15 min at 4°C to pellet the IBs.

Solubilisation of IBs and refolding of $PilN_{41}$ and $PilO_{45}$ followed the procedure described in Ref. [33]. The

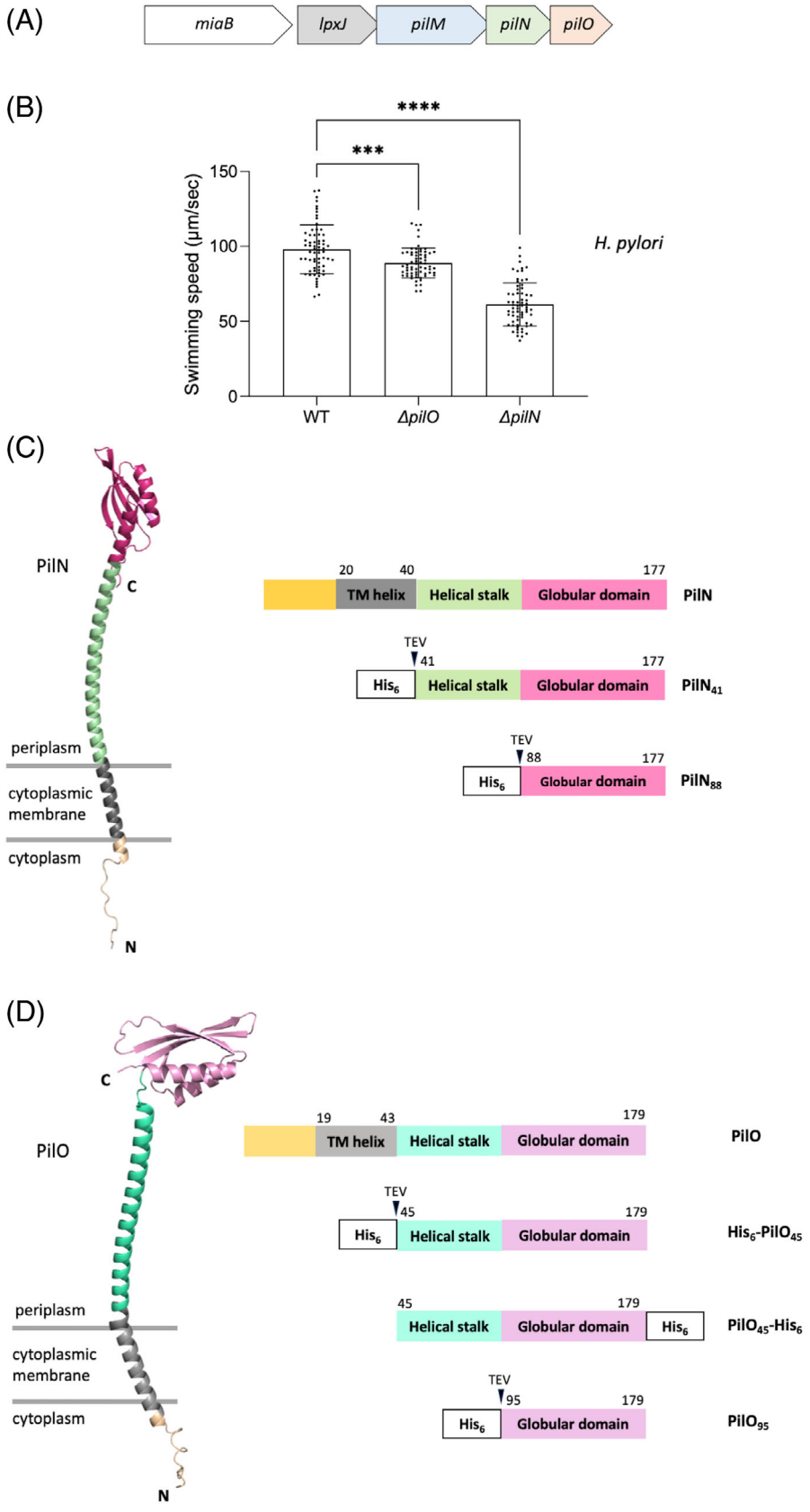

FIGURE 1 (A) The genomic organisation of the *pilMNO* locus in *H. pylori* (B) Swimming speeds of *H. pylori* SS1 WT and Δ*pilO::kan* and Δ*pilN::kan* mutants in liquid media BB10. For each strain, the speeds of 66 individual cells, the mean value and the standard deviation are shown. ***$p < .001$, ****$p < .0001$. Statistical analysis of differences in swimming speeds between the mutants and WT was carried out using one-way analysis of variance (ANOVA) followed by Dunnett's test to calculate P-values. The mean straight swimming speeds for the WT and Δ*pilO* and Δ*pilN* mutants were 97 ± 16, 88 ± 9 and 61 ± 14 µm/s, respectively. (C, D) Predicted structures and membrane topologies of *H. pylori* PilN (A) and PilO (B) and schematics of full-length proteins and the soluble variants used in this study. TEV, tobacco etch virus protease cleavage site.

refolded protein was loaded onto a 5 mL HiTrap Chelating HP column (Cytiva) equilibrated with buffer B (200 mM NaCl, 20 mM Tris–HCl, pH 8.0, 10 mM imidazole), and following a wash with the same buffer, eluted with buffer C (200 mM NaCl, 20 mM Tris–HCl pH 8.0, 500 mM imidazole), concentrated and passed

through a Superdex 75 HiLoad 26/60 size exclusion column (GE Healthcare) in buffer D (20 mM CHES, pH 10.5, 150 mM NaCl). Recombinant $PilN_{88}$ and $PilO_{95}$ were purified by following the procedure described in Ref. [34], the size exclusion chromatography step was the same as for $PilN_{41}$ and $PilO_{45}$. The molecular weight (MW) was determined from the calibration plot of log(MW) versus retention volume: $V_{retention}$ (mL) = 631.3–104.3 × log(MW).[35]

Far-UV circular dichroism (CD) spectra were obtained using a JASCO J600 spectropolarimeter (wavelength range 200–250 nm; scan rate 20 nm/min, optical path length 2 mm). The spectra were recorded in triplicate and then averaged. Refolded and purified $PilN_{41}$ (0.1 mg/mL) was analysed in two buffers, one containing 10 mM sodium phosphate pH 7.0, and the other containing 20 mM CHES pH 10.5, 150 mM NaCl. The BeStSel server[36] was used to deduce the secondary structure content of the protein by fitting the ellipticity data. The prediction of secondary structure based on the amino acid sequence was performed using the Jpred4 server (http://www.compbio.dundee.ac.uk/www-jpred/).[37]

3 | RESULTS

3.1 | *H. pylori* SS1 Δ*pilN* and Δ*pilO* mutants swim slower than WT in liquid media

To assess if the loss of PilO or PilN function affects the rotational speed of the flagellar motor in *H. pylori* strain SS1, we generated isogenic Δ*pilN::kan* and Δ*pilO::kan* mutant strains by replacing the middle part of either gene with the kanamycin resistance gene *aphA3* and measured their linear swimming speeds in BB10 using bright-field optical microscopy. The mean straight swimming speeds for the WT cells and Δ*pilO* and Δ*pilN* mutants were 97 ± 16, 88 ± 9 and 61 ± 14 μm/s, respectively (Figure 1B). The straight swimming speed for WT is comparable to the maximum linear speed recorded for this strain,[38] because the data were filtered to only include cells that swam in linear fashion for at least 0.5 s. The motility of the Δ*pilN* mutant in liquid media was significantly impaired as compared to WT (30% reduction in linear swimming speed), while insertional inactivation of the *pilO* gene resulted in only a small (9%), albeit statistically significant ($p < .001$), reduction in swimming speed. It has been previously reported that there is a correlation between the swimming speed and rotational speed of the flagellar motor.[39] We therefore speculate that the observed linear speed reduction is likely to be caused by the reduction in the rotational speed of the flagellar motor, suggesting that the loss of functional PilN or PilO affected the generation of force in the flagellar motor.

3.2 | Recombinant *H. pylori* PilN lacking transmembrane helix forms dimers

H. pylori PilN and PilO are predicted to have similar topologies: each contains an N-terminal transmembrane (TM) helix (with the protein's N-terminus in the cytoplasm), connected to a C-terminal globular periplasmic domain via a helical stalk (Figure 1C,D). To produce and characterize their soluble variants, we first expressed genes encoding PilN and PilO that lack the TM helix ($PilN_{41}$ and $PilO_{45}$) (Figure 1C,D) in *E. coli*. The cells produced these recombinant proteins in inclusion bodies, from which only $PilN_{41}$ could be recovered by refolding. Our initial attempt to purify $PilN_{41}$ using Ni-NTA affinity chromatography resulted in extensive precipitation. The likely cause was that the high ionic strength (500 mM NaCl) of the standard Ni-NTA buffers created unfavourable conditions for the $PilN_{41}$ protein, the hydrophobic amino-acid content of which is high (40%; $PilN_{88}$ and $PilO_{95}$ similar). Indeed, reduction of the NaCl concentration in Ni-NTA buffers to 200 mM improved the protein solubility and yield. We then assessed the protein solubility in different buffers by measuring the maximum concentration that could be achieved using centrifugal ultrafiltration. We found that the protein solubility increased dramatically when pH was shifted to highly alkaline (pH 10.5) (Figure 2A). While the consideration of the isoelectric point (pI = 6.0) alone cannot explain the requirement for such a high pH, analysis of the predicted structure of $PilN_{41}$ revealed two dense clusters of residues with basic side chains (Arg (p*K*a = 12.5), Lys (p*K*a = 10.5), His (p*K*a = 6.0)) (Figure 2A). These likely destabilise the fold of isolated $PilN_{41}$ at pH < 10.5.

To test this hypothesis, we investigated the secondary structure of refolded and purified $PilN_{41}$ at pH 7.0 and pH 10.5 using CD. Estimation of the α-helix and β-sheet content from the CD spectrum recorded at pH 10.5 (Figure 3A) gave values (38% α, 18% β) that were very close to those predicted from the sequence analysis (40% α, 17% β), indicating that $PilN_{41}$ extracted from the inclusion bodies was folded at this pH. In contrast, in the pH 7.0 buffer, the protein secondary structure contained only 5% α and 16% β (Figure 3B), confirming that reducing pH destabilises the fold of $PilN_{41}$.

We then determined the oligomeric state of $PilN_{41}$ using size exclusion chromatography of the highly

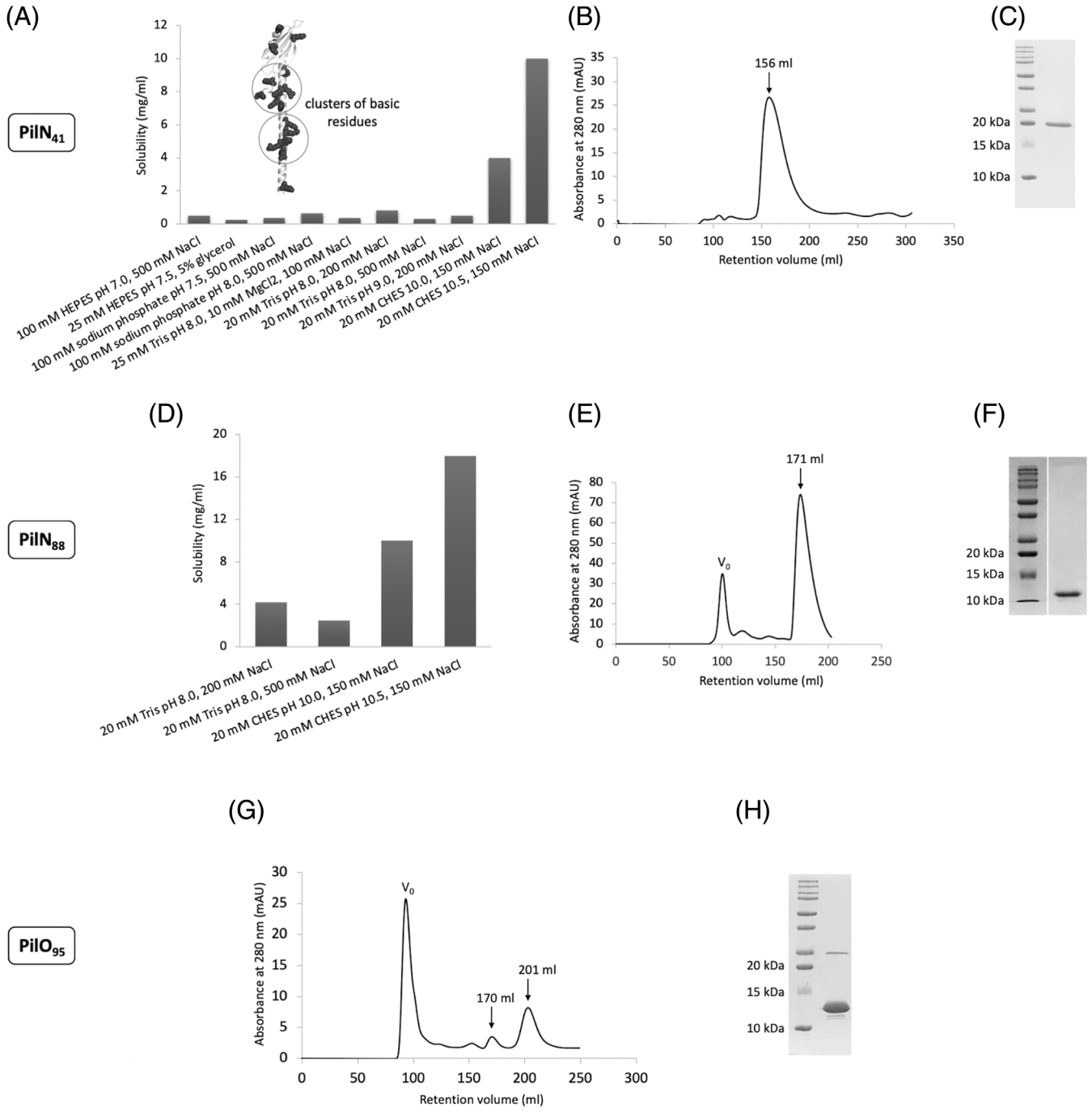

FIGURE 2 Biochemical characterisation of soluble forms of *H. pylori* PilN and PilO. (A) Isolated $PilN_{41}$ is soluble under alkaline conditions because of the clusters of residues with basic side chains that destabilise the fold at pH < 10.5. (B,E,G) Gel filtration traces of purified $PilN_{41}$, $PilN_{88}$ and $PilO_{95}$ (peaks corresponding to monomers, dimers or aggregates that elute in the void volume V_o are labelled). (C,F,H) Achieved purity of $PilN_{41}$, $PilN_{88}$ and $PilO_{95}$ (Coomassie Blue-stained 15% SDS-PAGE gels).

purified protein. $PilN_{41}$ eluted as a single peak (Figure 2B) corresponding to MW ≈ 36.1 kDa. The calculated MW of the $PilN_{41}$ monomer is 20.1 kDa, which suggested that $PilN_{41}$ is a dimer in solution. Approximately 3 mg of pure $PilN_{41}$ (Figure 2C) was obtained from 1 L of bacterial culture.

3.3 | Globular C-terminal domains of *H. pylori* PilN and PilO also form dimers in solution

Aiming to produce a soluble form of the periplasmic domain of PilO, we redesigned the construct aiming to

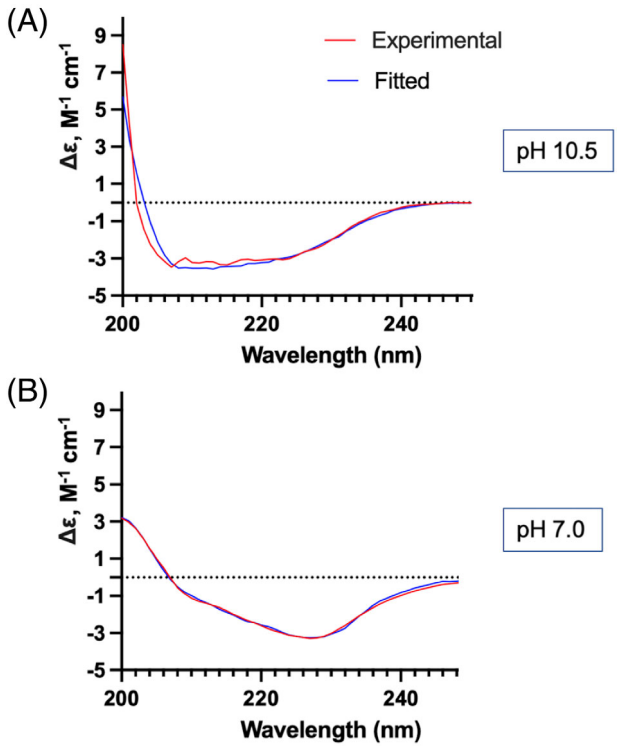

FIGURE 3 Far-UV CD spectra of $PilN_{41}$ (0.1 mg/mL) prepared in (A) pH 7.0 buffer and (B) pH 10.5 buffer. Analysis of this data using the BeStSel server shows that at pH 10.5, the secondary structure of $PilN_{41}$ contained 38% α, 18% β and 44% random coil, consistent with the folded state. At pH 7.0, the secondary structure contained 5% α, 16% β and 79% random coil, indicative of a protein fold that has become destabilised.

express only the PilO globular, α/β sandwich-type domain, named $PilO_{95}$ (Figure 1D), with the boundaries matching those of the soluble, crystallisable domain of PilO from *Pseudomonas aeruginosa* ($PilO_{\Delta 109}$[37]). We also produced the construct for the expression of the globular, α/β sandwich-type domain of PilN, $PilN_{88}$, by following the same principle (Figure 1C). This strategy significantly increased the recombinant proteins solubility in the *E. coli* cytoplasm, and the expression conditions were optimised to yield the highest levels of soluble $PilN_{88}$ and $PilO_{95}$ (16°C, overnight induction with 0.1 mM IPTG). The solubility of purified $PilN_{88}$ in several tested buffers was also higher than that of isolated $PilN_{41}$ (Figure 2D), confirming that removing the long helical stalk stabilised the protein. According to the results of the size exclusion experiments, $PilN_{88}$ was predominantly dimeric (MW ≈ 25.9 kDa, twice the calculated MW of the monomer = 13.9 kDa) (Figure 2E). In contrast, a significant fraction of $PilO_{95}$ (calculated MW = 13.6 kDa) eluted as a monomer (MW ≈ 13.3 kDa), although a dimer (MW ≈ 26.5 kDa) and higher oligomeric species were also present (Figure 2G). $PilN_{88}$ and $PilO_{95}$ were purified using a combination of Ni-NTA affinity and size exclusion chromatography to >95% electrophoretic homogeneity based on Coomassie Blue staining of the SDS-PAGE gels (Figure 2F,H) with the yields of 0.5 and 0.2 mg of pure protein per 1 L of bacterial culture.

4 | DISCUSSION

Following up on the recent discovery that the *H. pylori* genome encodes proteins homologous to Type IV pilus alignment proteins PilM, PilN and PilO,[25–29] and that inactivation of PilO changes bacterial motility in semi-solid media,[25] we addressed the question of whether PilO, and the protein that is intimately associated with PilO in the Type IV system (PilN) have a direct functional link with the bacterial flagellar motor. We demonstrated that mutation of the *pilO* or *pilN* gene in *H. pylori* strain SS1 reduced the mean linear swimming speed of the cells in liquid media. This observation indicates that the previously observed soft-agar phenotype cannot be explained by altered chemotactic behaviour—the loss of PilN or PilO function likely affects the rotational speed of the flagellar motor, possibly due to loss of direct or mediated interactions with its force-generating component, the stator. While this study was under review, it was reported that PilN and PilO do, in fact, form part of the *H. pylori* flagellar motor,[40] and that they were found among immunoaffinity-purified MotB coisolates,[40] which supports our conclusion. Interestingly, no statistically significant difference was observed between the swimming speeds of WT cells and *pilO* mutants in *H. pylori* strain G27,[40] which contrasts the outcome of our study. This can possibly be explained by the differences in how the *pilO* mutants were designed (in this study, the first and the last 100 bp of the SS1 *pilO* gene were retained, while the G27 mutant had only 24 bp and 19 bp of the original gene remaining at the 5′ and 3′ ends, respectively). We have previously illustrated that for a different component of the flagellar motor, FliL, the resulting motility phenotype of deletion mutants depends on what part of the *fliL* gene was deleted.[41] A similar phenomenon may occur here with different *pilO* mutants.

H. pylori does not have Type IV pili, but it may have acquired genes encoding the Type IV pilus alignment complex from a different species and adapted it to enhance or to regulate a completely different membrane-embedded molecular machine—the flagellar motor. We produced the soluble variants of PilN and PilO and demonstrated that they share some common key biochemical properties with their Type IV pili counterparts[42–44]: (1) they are able to form homodimers; (2) the helical stalk is not required for homodimerisation; and (3) the

homodimer formed by the globular C-terminal domain of PilN is more stable than the corresponding PilO homodimer. The design with the cleavable affinity tag makes these constructs suitable for future structural and biophysical studies aimed at elucidation of the molecular mechanism of their adapted function in the bacterial flagellar motor.

ACKNOWLEDGEMENTS

We thank Karen Ottemann and Xiaolin Liu (University of California Santa Cruz) for critically reading the manuscript. Open access publishing facilitated by Monash University, as part of the Wiley - Monash University agreement via the Council of Australian University Librarians.

FUNDING INFORMATION

This work was supported by the Australian Research Council grant DP210103056 to A.R.

ORCID

Anna Roujeinikova https://orcid.org/0000-0001-8478-4751

REFERENCES

1. Hooi JKY, Lai WY, Ng WK, Suen MMY, Underwood FE, Tanyingoh D, et al. Global prevalence of *Helicobacter pylori* infection: systematic review and meta-analysis. Gastroenterology. 2017;153:420–9.
2. Warren JR, Marshall B. Unidentified curved bacilli on gastric epithelium in active chronic gastritis. Lancet. 1983;1:1273–5.
3. Forman D et al. An international association between *helicobacter pylori* infection and gastric cancer. The EUROGAST Study Group. Lancet. 1993;341:1359–62.
4. Peek RM Jr, Blaser MJ. *Helicobacter pylori* and gastrointestinal tract adenocarcinomas. Nat Rev Cancer. 2002;2:28–37.
5. de Martel C, Georges D, Bray F, Ferlay J, Clifford GM. Global burden of cancer attributable to infections in 2018: a worldwide incidence analysis. Lancet Glob Health. 2020;8:e180–90.
6. Sung H, Ferlay J, Siegel RL, Laversanne M, Soerjomataram I, Jemal A, et al. Global cancer statistics 2020: GLOBOCAN estimates of incidence and mortality worldwide for 36 cancers in 185 countries. CA Cancer J Clin. 2021;71:209–49.
7. Evans DG, Queiroz DM, Mendes EN, Evans DJ Jr. *Helicobacter pylori cagA* status and *s* and *m* alleles of *vacA* in isolates from individuals with a variety of *H. pylori*-associated gastric diseases. J Clin Microbiol. 1998;36:3435–7.
8. Tohidpour A, Gorrell RJ, Roujeinikova A, Kwok T. The middle fragment of *Helicobacter pylori* CagA induces Actin rearrangement and triggers its own uptake into gastric epithelial cells. Toxins (Basel). 2017;9:237.
9. Roujeinikova A. Phospholipid binding residues of eukaryotic membrane-remodelling F-BAR domain proteins are conserved in *Helicobacter pylori* CagA. BMC Res Notes. 2014;7:525.
10. Krulwich TA, Sachs G, Padan E. Molecular aspects of bacterial pH sensing and homeostasis. Nat Rev Microbiol. 2011;9:330–43.
11. Modak JK, Rut W, Wijeyewickrema LC, Pike RN, Drag M, Roujeinikova A. Structural basis for substrate specificity of *Helicobacter pylori* M17 aminopeptidase. Biochimie. 2016;121:60–71.
12. Stent A, Every AL, Sutton P. *Helicobacter pylori* defense against oxidative attack. Am J Physiol Gastrointest Liver Physiol. 2012;302:G579–87.
13. Ud-Din AI, Liu YC, Roujeinikova A. Crystal structure of *Helicobacter pylori* pseudaminic acid biosynthesis N-acetyltransferase PseH: implications for substrate specificity and catalysis. PLoS One. 2015;10:e0115634.
14. Hanyu H, Engevik KA, Matthis AL, Ottemann KM, Montrose MH, Aihara E. *Helicobacter pylori* uses the TlpB receptor to sense sites of gastric injury. Infect Immun. 2019;87:e00202–19.
15. Hu S, Ottemann KM. *Helicobacter pylori* initiates successful gastric colonization by utilizing L-lactate to promote complement resistance. Nat Commun. 2023;14:1695.
16. Machuca MA, Johnson KS, Liu YC, Steer DL, Ottemann KM, Roujeinikova A. *Helicobacter pylori* chemoreceptor TlpC mediates chemotaxis to lactate. Sci Rep. 2017;7:14089.
17. Qin Z, Lin WT, Zhu S, Franco AT, Liu J. Imaging the motility and chemotaxis machineries in *Helicobacter pylori* by cryo-electron tomography. J Bacteriol. 2017;199:e00695-16.
18. Zhou X, Roujeinikova A. The structure, composition, and role of periplasmic stator scaffolds in polar bacterial flagellar motors. Front Microbiol. 2021;12:639490.
19. Tachiyama S, Chan KL, Liu X, Hathroubi S, Peterson B, et al. The flagellar motor protein FliL forms a scaffold of circumferentially positioned rings required for stator activation. Proc Natl Acad Sci U S A. 2022;119:e2118401119.
20. Reboul CF, Andrews DA, Nahar MF, Buckle AM, Roujeinikova A. Crystallographic and molecular dynamics analysis of loop motions unmasking the peptidoglycan-binding site in stator protein MotB of flagellar motor. PLoS One. 2011;6:e18981.
21. Andrews DA, Nesmelov YE, Wilce MC, Roujeinikova A. Structural analysis of variant of *Helicobacter pylori* MotB in its activated form, engineered as chimera of MotB and leucine zipper. Sci Rep. 2017;7:13435.
22. O'Neill J, Xie M, Hijnen M, Roujeinikova A. Role of the MotB linker in the assembly and activation of the bacterial flagellar motor. Acta Crystallogr D Biol Crystallogr. 2011;67:1009–16.
23. Beeby M, Ribardo DA, Brennan CA, Ruby EG, Jensen GJ, Hendrixson DR. Diverse high-torque bacterial flagellar motors assemble wider stator rings using a conserved protein scaffold. Proc Natl Acad Sci U S A. 2016;113:E1917–26.
24. Eppinger M, Baar C, Raddatz G, Huson DH, Schuster SC. Comparative analysis of four campylobacterales. Nat Rev Microbiol. 2004;2:872–85.
25. Sagoo J, Abedrabbo S, Liu X, Ottemann KM. Discovery of type IV filament membrane alignment complex homologs in *H. pylori* that promote soft-agar migration. bioRxiv [Preprint]. 2023. https://doi.org/10.1101/2023.04.27.537399
26. Sharma CM, Hoffmann S, Darfeuille F, Reignier J, Findeiss S, et al. The primary transcriptome of the major human pathogen *Helicobacter pylori*. Nature. 2010;464:250–5.
27. Tammam S, Sampaleanu LM, Koo J, Manoharan K, Daubaras M, Burrows LL, et al. PilMNOPQ from the

Pseudomonas aeruginosa type IV pilus system form a transenvelope protein interaction network that interacts with PilA. J Bacteriol. 2013;195:2126–35.
28. Chang YW, Rettberg LA, Treuner-Lange A, Iwasa J, Søgaard-Andersen L, Jensen GJ. Architecture of the type IVa pilus machine. Science. 2016;351:aad2001.
29. Craig L, Forest KT, Maier B. Type IV pili: dynamics, biophysics and functional consequences. Nat Rev Microbiol. 2019;17:429–40.
30. Tsirigos KD, Peters C, Shu N, Kall L, Elofsson A. The TOPCONS web server for consensus prediction of membrane protein topology and signal peptides. Nucleic Acids Res. 2015;43:W401–7.
31. Jumper J, Evans R, Pritzel A, Green T, Figurnov M, Ronneberger O, et al. Highly accurate protein structure prediction with AlphaFold. Nature. 2021;596:583–9.
32. Mirdita M, Schütze K, Moriwaki Y, Heo L, Ovchinnikov S, Steinegger M. ColabFold: making protein folding accessible to all. Nat Methods. 2022;19:679–82.
33. Liu YC, Roujeinikova A. Expression, refolding, purification and crystallization of the sensory domain of the TlpC chemoreceptor from *Helicobacter pylori* for structural studies. Protein Expr Purif. 2015;107:29–34.
34. Woon AP, Tohidpour A, Alonso H, Saijo-Hamano Y, Kwok T, Roujeinikova A. Conformational analysis of isolated domains of *Helicobacter pylori* CagA. PLoS One. 2013;8:e79367.
35. Aydin I, Dimitropoulos A, Chen SH, Thomas C, Roujeinikova A. Purification, crystallization and preliminary X-ray crystallographic analysis of the putative *Vibrio parahaemolyticus* resuscitation-promoting factor YeaZ. Acta Crystallogr Sect F Struct Biol Cryst Commun. 2011;67:604–7.
36. Micsonai A, Wien F, Kernya L, Lee YH, Goto Y, Réfrégiers M, et al. Accurate secondary structure prediction and fold recognition for circular dichroism spectroscopy. Proc Natl Acad Sci U S A. 2015;112:e3095–103.
37. Drozdetskiy A, Cole C, Procter J, Barton GJ. JPred4: a protein secondary structure prediction server. Nucleic Acids Res. 2015;43:W389–94.
38. Aihara E, Closson C, Matthis AL, Schumacher MA, Engevik AC, Zavros Y, et al. Motility and chemotaxis mediate the preferential colonization of gastric injury sites by *Helicobacter pylori*. PLoS Pathog. 2014;10:e1004275.
39. Magariyama Y, Sugiyama S, Muramoto K, Kawagishi I, Imae Y, Kudo S. Simultaneous measurement of bacterial flagellar rotation rate and swimming speed. Biophys J. 1995;69:2154–62.
40. Liu X, Tachiyama S, Zhou X, Mathias RA, Bonny SQ, Khan MF, et al. Bacterial flagella hijack type IV pili proteins to control motility. Proc Natl Acad Sci U S A. 2024;121:2317452121.
41. Liu X, Roujeinikova A, Ottemann K. FliL functions in diverse microbes to negatively modulate motor output via its N-terminal region. MBio. 2023;14:e0028323.
42. Leighton TL, Mok MC, Junop MS, Howell PL, Burrows LL. Conserved, unstructured regions in *Pseudomonas aeruginosa* PilO are important for type IVa pilus function. Sci Rep. 2018;8:2600.
43. Sampaleanu LM, Bonanno JB, Ayers M, Koo J, Tammam S, Burley SK, et al. Periplasmic domains of *Pseudomonas aeruginosa* PilN and PilO form a stable heterodimeric complex. J Mol Biol. 2009;394:143–59.
44. Leighton TL, Yong DH, Howell PL, Burrows LL. Type IV pilus alignment subcomplex proteins PilN and PilO form homo- and heterodimers in vivo. J Biol Chem. 2016;291:19923–38.

How to cite this article: Bonny SQ, Zhou X, Khan MF, Rahman MM, Xin Y, Vankadari N, et al. Functional and biochemical characterisation of remote homologues of type IV pili proteins PilN and PilO in *Helicobacter pylori*. IUBMB Life. 2024;76(10):780–7. https://doi.org/10.1002/iub.2828